

Illustrative Rendering of Vortex Cores

Sohail Shafii¹, Harald Obermaier,¹ Václav Kolář,² Mario Hlawitschka,³ Christoph Garth,⁴ Bernd Hamann,¹ and Kenneth I. Joy¹

¹Institute for Data Analysis and Visualization, Department of Computer Science, University of California, Davis, U.S.A.

²Institute of Hydrodynamics; Academy of Sciences of the Czech Republic

³Institute of Computer Science; Universität Leipzig, Germany

⁴Computational Topology Group; University of Kaiserslautern, Germany

Abstract

Vortices are features crucial for understanding transitional and turbulent flow fields, and have often been visualized using isosurfaces, hulls, and line-like structures. However, they have not been represented in a non-photorealistic manner that intuitively reflects their local characteristics. We introduce a novel visualization method that represents these features as illustrative vortex cores, and show how this illustrative method clearly depicts vortex properties such as direction, rotational strength, spatial extension, and underlying flow behavior simultaneously, in a fashion superior to standard visualization approaches. Our non-photorealistic visualizations leverage the axis and rotational properties of a vortex detector to depict the direction and the rotational strength of vortices, respectively. Furthermore, we extract flow behavior in the vicinity of the vortex cores to provide context for the vortices that we extract. We demonstrate the efficacy of our illustrative vortex extraction framework in two commonly used data sets by showing how they characterize the properties of the examined flow fields.

Categories and Subject Descriptors (according to ACM CCS): Computer Graphics [I.3.8]: Applications—Picture/Image Generation [I.3.3]: Line and curve generation—

1. Introduction

Extracting and visualizing *vortices* in flow fields is an important problem in flow field analysis, as they are crucial for the study of fluid dynamics and mixing. There exist multiple definitions of vortices based on various properties [JMT05], and they are often represented using surfaces, lines, or hulls. While there are illustrative methods in the flow literature [JL97, LS07, EBRI09, BWF*10, JR05, HGH*10], there is a lack of published approaches that apply these intuitive, non-photorealistic depictions to portray vortex cores' mathematical traits. For this purpose, we introduce an illustrative, line-based extraction method that depicts the directional, rotational, spatial, and flow-related properties of vortices in a more transparent manner compared to standard vortex visualization approaches.

The initial step of our illustrative vortex extraction framework requires a criterion that encodes rotational and directional properties of vortices. We use a kinematic detector known as the “corotation of line segments” or “corotation” [KMS10]. We pair this criterion with a predictor-corrector approach [BS95, SRE05] to extract vortex core lines, each with spatial extent represented by a *vortex hull*,

and extend this approach by using illustrative rendering techniques. We depict ribbons to visualize vortex rotational strength and vortex direction, and we scale each ribbon based on the vortex hull size. Furthermore, we render illustrative flow lines in the vicinity of each vortex to depict complex flow behaviors underneath a vortex's surface. The research contributions provided by our extraction and visualization framework are:

- An application of illustrative rendering techniques to vortex extraction
- A novel illustration of vortex characteristics such as rotational strength, direction, and extent
- A delineation of flow information to provide context for each vortex

Vortex detection and illustrative flow rendering are introduced in Section 2. Our methods are explained in Sections 3, and their corresponding results are shown in Section 4. Future research possibilities are covered in Section 5.

2. Background

There exists a wealth of region-type and line-based vortex-detection techniques that allows one to extract and visualize vortices. Region-type techniques are typically based on local operators such as the Q [HWM88], Δ [Dal83, VKM83], λ_2 [JH95], and residual vorticity [Kol07, KMS10] criteria. Line-based techniques extract global vortex features dependent on the directional component of vortices, including the parallel vectors operator and similar methods [SH95, FPH*08], predictor-corrector [BS95], and ridge or valley line methods [SWH05, SWTH07]. A summary of vortex detection methods is provided by Jiang *et al.* [JMT05]. Vortices are discussed in the context of feature extraction and tracking by Post *et al.* [PVH*03], and analyzed by [SPP04, SPS06].

We extract vortex core lines and hulls by adapting a predictor-corrector technique [SWE06, SVG*08, BSER09] devised by Stegmaier *et al.* [SRE05]. Our predictor-corrector adaptation is paired with corotation (i.e., planar residual vorticity associated with local “rigid-body rotation”) and related vectors [KMS10]. We use points that have positive (strong) corotation values and that are local maxima as seeds for vortex core line integration. Our algorithm integrates vortex core lines based on corotation orientation vectors, and corrects each point of integration to maximize the corotation value in the plane perpendicular to the integration direction. By using sampling rays at each integration point, one can measure the radial extents of the region that the vortex core line exists inside of, and measure cross-sectional areas of the region to determine if the area is too small for integration. Vortex cross sections can be used to recreate the vortex regions as *hulls* using a discrete Fourier series as specified by [SRE05]. Since these types of hulls could experience self-intersections, we recreate smoother versions using metaball surfaces [Bli82] based on the average radial values associated with each cross section [SOL*13]. In general, any line-based extraction approach that encodes vortex rotation strength, extent, and direction would be suitable for this feature extraction phase.

While it is simple to create vortex core lines to portray vortex axes, vortex core hulls to indicate vortex extent [JMT05], and line integral convolution (LIC) [CL93] surfaces to depict flow [SWE06], there is a limited application of illustrative techniques that expand on these representations. There are many examples where illustrative rendering methods are used to represent general flow information [BCP*12], such as uniformly spaced streamlines for 2D [JL97] or 3D flows [LS07]. While the latter method produces appealing results in our data sets, its dependence on the view requires an integration of streamlines whenever the view is changed, which can slow down interactivity.

Everts *et al.* [EBRI09] introduced an alternative line-rendering technique that uses view-dependent halos around streamlines and other methods to efficiently visualize a

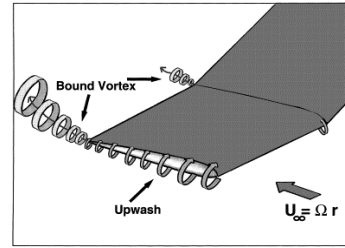


Figure 1: Example of wing-bound vortices related to lift experienced by a wing, courtesy of [DSFJ00]. This illustration effectively depicts standard vortex properties such as rotation, axis of orientation, and extent, together with a visual indicator regarding the inflow of air.

dense rendering of streamlines. We chose to render illustrative tubes in the vicinity of the vortex cores, as they can be densely packed due to their thickness, and can be delineated using silhouette-rendering. There are also methods that extract illustrative stream surfaces, ribbon-like “cuts” or “slabs,” as demonstrated by Hummel *et al.* [HGH*10], Born *et al.* [BWF*10], and Edmunds *et al.* [ELM*12]. In our work, we use illustrative ribbons with arrow-heads to effectively display rotational behaviors of vortex core lines, and we orient them according to vortex directions.

3. Illustrative Rendering of Vortex Cores

We list the following fundamental vortex properties that are used to develop our illustrative rendering techniques, many of which have been defined by vortex detectors:

- Mathematical vortex descriptors:
 - Rotational strength, such as residual vorticity [Kol07, KMS10]
 - Axis of orientation, such as vorticity direction [SRE05]
 - Region of extent, often represented by hulls [SRE05, SWE06, BSER09]
- Contextual flow information [JL97, LS07, EBRI09]

In the literature, illustrations such as the one shown in Figure 1 are examples of intuitive portrayals that encode some of the vortex properties listed above. Rotational strength indicators allow one to isolate strong or weak regions inside a vortex. The axis of orientation and region of extent properties reflect directional and hull-like properties of vortices, allowing one to represent them as global turbulent features inside of a data set. Since vortices may often exist in steady rotational flow or in strong translational flow, it is necessary to visualize flow information in the region corresponding to the vortex. An example of how our approach typifies the above aspects is shown in Figure 2, where we show that typical visualizations fail to depict the same quantity of information.

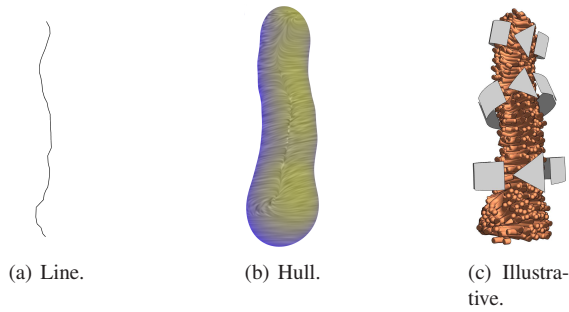


Figure 2: Visualization of vortex core behavior with standard methods, shown in 2(a) (vortex core line) and 2(b) (vortex core hull with LIC and shading developed by [GGSC98]), and our illustrative approach, shown in 2(c). The hull only indicates direction, extent, and tangential flow. The illustrative approach depicts rotational strength (weak: broken ribbons, strong: continuous ribbons) of sample points relative to the entire vortex, and extent via the sizes of the ribbons. Arrow heads indicate rotational direction, and the flow tubes produce a compact visualization of vortex flow information beyond tangential surface velocities.

3.1. Illustrative Ribbons

To represent the basic mathematical properties of our vortices, we construct illustrative ribbons that provide a natural visualization of each vortex’s rotational strength, axis of rotation, and extent, as seen in Figure 2(c).

We first create circular line strips spaced evenly along a vortex core line, and extend them into ribbons using a geometry shader. Since a vortex core line direction might change abruptly from point to point, the axis of orientation of each line strip is the average of the vortex core line’s segment that corresponds to the ribbon’s origin, and the neighboring segments that are ahead and behind that segment. When the segment is at the beginning or end of the vortex core line, the neighboring segment after or before the segment is used for averaging, respectively.

The radius of the line strip corresponds to the vortex hull’s average radius at the ribbon’s origin, and encodes spatial extent. If the interpolated residual vorticity magnitude at the ribbon’s origin is weak relative to the maximum scalar value along the vortex core line, the line strip will be broken into smaller portions in the geometry shader to intuitively convey relative rotational speed. A line strip with larger or complete portions indicates that the scalar value is high relative to the maximum. Thus, a ribbon with ten segments corresponds to a smaller rotational value relative to a ribbon with five, two or one segment. The size of the ribbons, along with their representation as dashed segments, allow us to qualitatively visualize the region containing the vortices and rotational strength attributes, respectively.

The circular line strips also contain a one-dimensional texture coordinate that indicates how far a point is along the strip. This approach allows us to create an arrow head at the end of the line strip, providing a clear indication of rotation direction. To create a hand-drawn appearance, we render silhouettes of our ribbons by rendering the mesh of the ribbons, and subsequently rendering its opaque geometry in a second pass. The meshes are offset into the depth buffer so that they do not occlude the opaque rendering. In addition, we color the ribbon back faces a darker color in a fragment shader to make them clearly distinguishable.

3.2. Illustrative Flow Indicators

We render flow tubes to provide contextual flow information inside vortices that go beyond flow behaviors on the surfaces of the hulls, as seen in Figure 2(c). It is important to define the locations of these flow tubes so that they are close to the core, but inside of the ribbons. The ribbons described in the previous section are scaled according to the vortex hull’s average radius, which is also used to create the metaball representation of the vortex hulls. The metaballs define individual scalar fields to create the isosurfaces of the vortex hulls. We apply thresholding on each metaball scalar field to define a mask that constrains the spatial extent of the integrated flow tubes. Like the ribbons, we render silhouettes of the tubes to provide a clear delineation of their shape properties.

4. Results

For evaluation, we have applied our illustrative vortex method to the blunt fin [HB85] ($39 \times 31 \times 31$ structured curvilinear grid) and delta wing (unstructured, approximately 3 million points) data sets. The former is a simulation of flow over a flat plane that encounters a blunt fin, while the latter describes vortex breakdown in aviation [GTS04]. The LIC shading shown here is based on [GGSC98].

We show a comparison of vortex hulls with LIC and our illustrative methods for the blunt fin data set in Figures 3(a) and 3(b). Unlike the LIC surfaces, the illustrative technique shows a dense 3D tube depiction of unsteady translational flow that exists underneath, and not just on the surface of the hulls. The ribbons portray the same regions as the hulls do, and their broken appearance also indicates the behavior of rotational values along the cores. For example, many of the sampled corotation values of the two large, diagonal vortices tend to be low compared to the maximum values found on each line, and are represented as ten-segment ribbons. Note that for the predictor-corrector method, the vortex core line can continue integrating in these weaker regions as long as the hull cross-sectional area is large enough. In the vortices parallel to the blunt object, five-segment ribbons are found, indicating a few instances where rotational strength is large. This non-photorealistic, intuitive representation of vortex’s rotational speed along a vortex core line is not available in the hull visualization.

A similar comparison between the LIC vortex hull method and our illustrative technique is shown in Figures 3(c) and 3(d) for the delta wing data set. One can observe the changes in rotational scalar values along the vortices by looking for one to two-segment (strong), five-segment (moderately strong) and ten-segment (weak) ribbons. Unlike the hull representation, we can see that the leftmost vortex that is closest to the viewer in 3(d) has strong rotation at the two-segment ribbon, while the rotational strength starts to taper off quickly as one moves along the vortex. Additionally, the illustrative flow tubes indicate a combination of translational and rotational flow inside of the vortex regions, while the LIC version only depicts tangential flow due to its integration in image-space.

The comparisons indicate that unlike traditional vortex visualization methods, our illustrative techniques unambiguously portray a vortex's rotational property, its direction of orientation, and its region of coverage. Additionally, our methods show flow field behavior inside of the regions covered by the hulls.

5. Conclusions

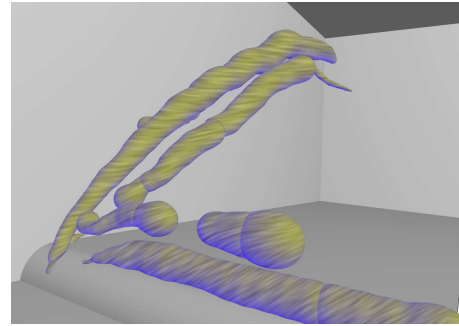
We have introduced an illustrative flow visualization framework that portrays a vortex's basic properties, together with related flow information. We compare our results against a typical hull-based representation of the same vortex core lines, and show the benefits of our approach. It is our plan to improve our results by allowing the user to view sections inside of the features extracted, similar to the method found in [BWF*10]. Additionally, we will investigate anisotropic shapes (such as ellipsoids) for vortex hull generation, which may be useful for more complex data sets compared to the ones used here.

6. Acknowledgements

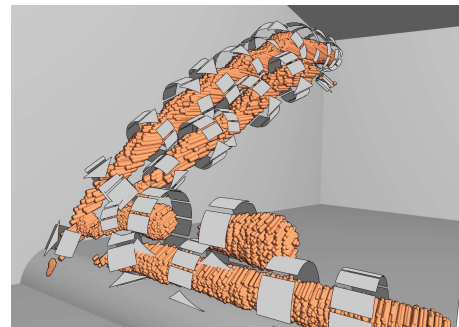
This work was partially supported by the Materials Design Institute, funded by the UC Davis/LANL Research Collaboration (LANL Agreement No. 75782-001-09). It was also supported by the NSF under contracts IIS 0916289 and IIS 1018097, the Office of Advanced Scientific Computing Research, Office of Science, of the US DOE under Contract No. DE-FC02-06ER25780 through the SciDAC programs VACET, and contract DE-FC02-12ER26072, SDAV Institute. V.K. acknowledges the support of ASCR through RVO: 67985874. We thank Simon Stegmaier for his code from [SRE05].

References

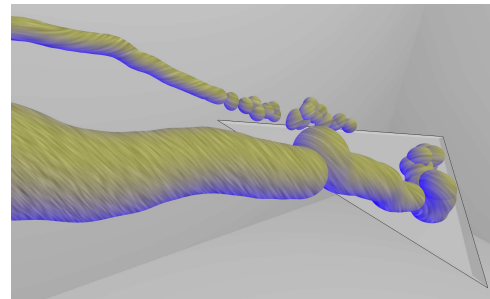
- [BCP*12] BRAMBILLA A., CARNECKY R., PEIKERT R., VIOLA I., HAUSER H.: Illustrative flow visualization: State of the art, trends and challenges. In *EuroGraphics 2012 State of the Art Reports* (2012), pp. 75–94. 2



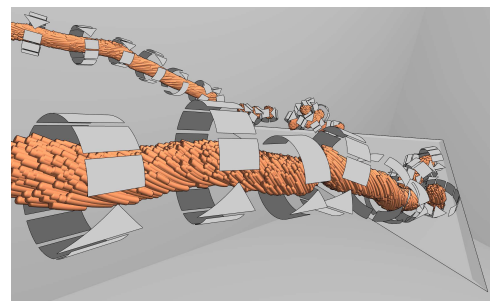
(a) Blunt fin; vortex hulls.



(b) Blunt fin; illustrative rendering.



(c) Delta wing; vortex hulls.



(d) Delta wing; illustrative rendering.

Figure 3: LIC-based vortex hull and illustrative renderings for the blunt fin (3(a)-3(b)) and delta wing data sets (3(c)-3(d)). The illustrative vortices depict direction and size of the vortices in a manner similar to the hulls. They also visualize flow behavior beneath the surfaces of the vortices and rotational strength, characteristics which are not available in the hull rendering.

- [Bli82] BLINN J. F.: A generalization of algebraic surface drawing. *ACM Trans. on Graphics* 1, 3 (July 1982), 235–256. 2
- [BS95] BANKS D. C., SINGER B. A.: A predictor-corrector technique for visualizing unsteady flow. *IEEE Trans. Vis. and Comput. Graphics* 1 (1995), 151–163. 1, 2
- [BSER09] BAYSAL K., SCHAFHITZEL T., ERTL T., RIST U.: Extraction and visualization of flow features. In *Imaging Measurement Methods for Flow Analysis*, Nitsche W., Dobriloff C., (Eds.), vol. 106 of *Notes on Numerical Fluid Mechanics and Multidisciplinary Design*. Springer Berlin / Heidelberg, 2009, pp. 305–314. 2
- [BWF*10] BORN S., WIEBEL A., FRIEDRICH J., SCHEUERMANN G., BARTZ D.: Illustrative stream surfaces. *IEEE Trans. Vis. and Comput. Graphics* 16, 6 (Nov. 2010), 1329–1338. 1, 2, 4
- [CL93] CABRAL B., LEEDOM L.: Imaging vector fields using line integral convolution. In *Proc. of 20th Annual Conf. on Computer Graphics and Interactive Techniques* (New York, NY, USA, 1993), SIGGRAPH '93, ACM, pp. 263–270. 2
- [Dal83] DALLMANN U.: Topological structures of three-dimensional vortex flow separation. In *American Institute of Aeronautics and Astronautics, Fluid and Plasma Dynamics Conference, 16th, Danvers, MA* (1983). 2
- [DSFJ00] DINDAR M., SHEPHARD M. S., FLAHERTY J. E., JANSEN K.: Adaptive cfd analysis for rotorcraft aerodynamics. *Computer Methods in Applied Mechanics and Engineering* 189, 4 (2000), 1055–1076. 2
- [EBRI09] EVERTS M., BEKKER H., ROERDINK J., ISENBERG T.: Depth-dependent halos: Illustrative rendering of dense line data. *IEEE Trans. Vis. and Comput. Graphics* 15, 6 (Nov.-Dec. 2009), 1299–1306. 1, 2
- [ELM*12] EDMUNDS M., LARAMEE R. S., MALKI R., MASTERS I., CROFT T., CHEN G., ZHANG E.: Automatic stream surface seeding: A feature centered approach. In *Computer Graphics Forum* (2012), vol. 31, pp. 1095–1104. 2
- [FPH*08] FUCHS R., PEIKERT R., HAUSER H., SADLO F., MUIGG P.: Parallel vectors criteria for unsteady flow vortices. *IEEE Trans. Vis. and Comput. Graphics* 14 (2008), 615–626. 2
- [GGSC98] GOOCH A., GOOCH B., SHIRLEY P., COHEN E.: A non-photorealistic lighting model for automatic technical illustration. In *Proceedings of the 25th annual conference on Computer graphics and interactive techniques* (1998), SIGGRAPH '98, pp. 447–452. 3
- [GTS04] GARTH C., TRICOCHÉ X., SCHEUERMANN G.: Tracking of vector field singularities in unstructured 3d time-dependent datasets. In *Proc. of IEEE Conf. on Vis. '04* (2004), pp. 329–336. 3
- [HB85] HUNG C., BUNING P.: Simulation of blunt-fin-induced shock-wave and turbulent boundary-layer interaction. *Journal of Fluid Mechanics* 154, 1 (1985), 163–185. 3
- [HGH*10] HUMMEL M., GARTH C., HAMANN B., HAGEN H., JOY K. I.: Iris: Illustrative rendering for integral surfaces. *IEEE Trans. Vis. and Comput. Graphics* 16, 6 (Nov. 2010), 1319–1328. 1, 2
- [HWM88] HUNT J., WRAY A., MOIN P.: Eddies, stream, and convergence zones in turbulent flows. *Center for Turbulence Research Report CTR-S88* (1988), 193–208. 2
- [JH95] JEONG J., HUSSAIN F.: On the identification of a vortex. *Journal of Fluid Mechanics* 285 (1995), 69–94. 2
- [JL97] JOBARD B., LEFER W.: Creating evenly-spaced streamlines of arbitrary density. In *Visualization in Scientific Computing '97* (1997), pp. 43–56. 1, 2
- [JMT05] JIANG M., MACHIRAJU R., THOMPSON D.: Detection and visualization of vortices. In *The Visualization Handbook* (2005), Hansen C. D., Johnson C. R., (Eds.), Elsevier, Amsterdam, pp. 295–309. 1, 2
- [JR05] JOSHI A., RHEINGANS P.: Illustration-inspired techniques for visualizing time-varying data. In *Proc. of IEEE Conf. on Vis. '05* (Oct. 2005), pp. 679–686. 1
- [KMS10] KOLAR V., MOSES P., SISTEK J.: Local corotation of line segments and vortex identification. In *Proc. of 17th Australasian Fluid Mechanics Conf.* (2010), Mallinson G., Cater J., (Eds.). 1, 2
- [Kol07] KOLAR V.: Vortex identification: New requirements and limitations. *International Journal of Heat and Fluid Flow* 28, 4 (2007), 638–652. 2
- [LS07] LI L., SHEN H.-W.: Image-based streamline generation and rendering. *IEEE Trans. Vis. and Comput. Graphics* 13, 3 (May 2007), 630–640. 1, 2
- [PVH*03] POST F. H., VROLIJK B., HAUSER H., LARAMEE R. S., DOLEISCH H.: The state of the art in flow visualisation: Feature extraction and tracking. In *Computer Graphics Forum* (2003), vol. 22, pp. 775–792. 2
- [SH95] SUJUDI D., HAIMES R.: Identification of swirling flow in 3d vector fields. In *AIAA 12th Computational Fluid Dynamics Conf., Paper 95-1715* (1995). 2
- [SOL*13] SHAFII S., OBERMAIER H., LINN R., KOO E., HLAWITSCHKA M., GARTH C., HAMANN B., JOY K.: Visualization and analysis of vortex-turbine intersections in wind farms. *IEEE Trans. Vis. and Comput. Graphics*, PrePrints (2013). 2
- [SPP04] SADLO F., PEIKERT R., PARKINSON E.: Vorticity based flow analysis and visualization for pelton turbine design optimization. In *Proc. of IEEE Conf. on Vis. '04* (2004), pp. 179–186. 2
- [SPS06] SADLO F., PEIKERT R., SICK M.: Visualization tools for vorticity transport analysis in incompressible flow. *IEEE Trans. Vis. and Comput. Graphics* 12 (2006), 949–956. 2
- [SRE05] STEGMAIER S., RIST U., ERTL T.: Opening the can of worms: An exploration tool for vortical flows. In *Proc. of IEEE Conf. on Vis. '05*. (2005), pp. 463–470. 1, 2, 4
- [SVG*08] SCHAFHITZEL T., VOLLRATH J., GOIS J., WEISKOPF D., CASTELO A., ERTL T.: Topology-preserving λ_2 -based vortex core line detection for flow visualization. In *Computer Graphics Forum* (2008), vol. 27, pp. 1023–1030. 2
- [SWE06] SCHAFHITZEL T., WEISKOPF D., ERTL T.: Interactive investigation and visualization of 3d vortex structures. In *Electronic Proc. of International Sym. on Flow Vis.* (September 2006). 2
- [SWH05] SAHNER J., WEINKAUF T., HEGE H.: Galilean invariant extraction and iconic representation of vortex core lines. In *IEEE VGTC Symposium on Visualization* (2005), pp. 151–160. 2
- [SWTH07] SAHNER J., WEINKAUF T., TEUBER N., HEGE H.-C.: Vortex and strain skeletons in eulerian and lagrangian frames. *IEEE Trans. Vis. and Comput. Graphics* 13, 5 (Sept.-Oct. 2007), 980–990. 2
- [VKM83] VOLLMERS H., KREPLIN H., MEIER H.: Separation and vortical-type flow around a prolate spheroid-evaluation of relevant parameters. In *Proc. of the AGARD Symposium on Aerodynamics of Vortical Type Flows in Three Dimensions* (Rotterdam, The Netherlands, 1983). 2